



Design, synthesis, biological evaluation and X-ray crystal structure of novel classical 6,5,6-tricyclic benzo[4,5]thieno[2,3-d]pyrimidines as dual thymidylate synthase and dihydrofolate reductase inhibitors

Xin Zhang^a, Xilin Zhou^a, Roy L. Kisliuk^b, Jennifer Piraino^c, Vivian Cody^c, Aleem Gangjee^{a,*}

^a Division of Medicinal Chemistry, Graduate School of Pharmaceutical Sciences, Duquesne University, Pittsburgh, PA 15282, United States

^b University School of Medicine, Boston, MA 02111, United States

^c Hauptman-Woodward Medical Research Institute, 700 Ellicott Street, Buffalo, NY 14203, United States

ARTICLE INFO

Article history:

Received 10 February 2011

Revised 25 March 2011

Accepted 30 March 2011

Available online 9 April 2011

Keywords:

DHFR

TS

Dual

Inhibitor

ABSTRACT

Classical antifolates (**4–7**) with a tricyclic benzo[4,5]thieno[2,3-d]pyrimidine scaffold and a flexible and rigid benzoylglutamate were synthesized as dual thymidylate synthase (TS) and dihydrofolate reductase (DHFR) inhibitors. Oxidative aromatization of ethyl 2-amino-4-methyl-4,5,6,7-tetrahydro-1-benzothiophene-3-carboxylate (**±**)-**9** to ethyl 2-amino-4-methyl-1-benzothiophene-3-carboxylate **10** with 10% Pd/C was a key synthetic step. Compounds with 2-CH₃ substituents inhibited human (h) TS (IC₅₀ = 0.26–0.8 μM), but not hDHFR. Substitution of the 2-CH₃ with a 2-NH₂ increases hTS inhibition by more than 10-fold and also affords excellent hDHFR inhibition (IC₅₀ = 0.09–0.1 μM). This study shows that the tricyclic benzo[4,5]thieno[2,3-d]pyrimidine scaffold is highly conducive to single hTS or dual hTS-hDHFR inhibition depending on the 2-position substituents. The X-ray crystal structures of **6** and **7** with hDHFR reveal, for the first time, that tricyclics **6** and **7** bind with the benzo[4,5]thieno[2,3-d]pyrimidine ring in the folate binding mode with the thieno S mimicking the 4-amino of methotrexate.

© 2011 Elsevier Ltd. All rights reserved.

1. Introduction

Because of its critical importance in the biosynthesis of purine and pyrimidine nucleic acids, folate metabolism is an attractive target for chemotherapy. Antifolates that target folate metabolism have found clinical utility as antitumor, antimicrobial, and antiprotozoal agents.^{1–5} Among the folate dependent enzymes, thymidylate synthase (TS) and dihydrofolate reductase (DHFR) have been of particular interest. TS is a key enzyme in the de novo synthesis of 2'-deoxythymidine-5'-monophosphate (dTMP) from 2'-deoxyuridine-5'-monophosphate (dUMP).^{6,7} The reaction requires 5,10-methylenetetrahydrofolate (5,10-CH₂THF) as a cofactor for one carbon unit transfer and represents the only de novo pathway for intracellular dTMP synthesis. DHFR catalyzes the reduction of dihydrofolate to tetrahydrofolate, and is indirectly responsible for dTMP synthesis by maintaining the reduced folate pool.⁸

Raltitrexed (RTX),⁹ pemetrexed (PMX)¹⁰ and methotrexate (MTX)¹¹ (Fig. 1) are examples of TS and/or DHFR inhibitors used in the clinic. RTX, approved in several European countries, Australia, Canada, and Japan for the treatment of advanced colorectal cancer, is a TS inhibitor that undergoes rapid polyglutamylolation by the enzyme folylpolyglutamate synthetase^{12,13} (FPGS). PMX, in

combination with cisplatin, was approved for the treatment of malignant pleural mesothelioma and also for non-small cell lung cancer. With TS inhibition as the primary mechanism of action, PMX was reported to inhibit several other folate-dependent enzymes including DHFR, glycinamide ribonucleotide formyltransferase (GARFTase), and aminoimidazole carboxamideribonucleotide formyltransferase (AICARFTase).¹⁰ Similar to RTX, polyglutamylolation by FPGS is essential for the cytotoxicity of PMX.

Classical antifolates, such as RTX and PMX, that have an *N*-benzoyl-L-glutamic acid side chain usually function as substrates for FPGS, which leads to high intracellular concentrations of these antitumor agents and increases TS inhibitory activity for some antifolates (RTX, 60-fold and PMX 130-fold) compared to their monoglutamate forms.^{9,10,14,15} Although polyglutamylolation of certain antifolates (such as RTX and PMX) is necessary for their cytotoxic activity, it has also been implicated in toxicity to host cells, because of the longer cellular retention time of such polyanionic poly-glutamate metabolites.¹⁶ In addition, reduced expression of FPGS in tumor cells can lead to resistance to FPGS dependent classical antifolates such as PMX.^{17–19}

To circumvent the potential tumor resistance problems associated with FPGS, classical antifolates should have high enzyme inhibitory potency as their monoglutamate forms and not require polyglutamylolation by FPGS to exert their antitumor activity.^{20,21}

* Corresponding author. Tel.: +1 412 396 6070.

E-mail address: gangjee@duq.edu (A. Gangjee).

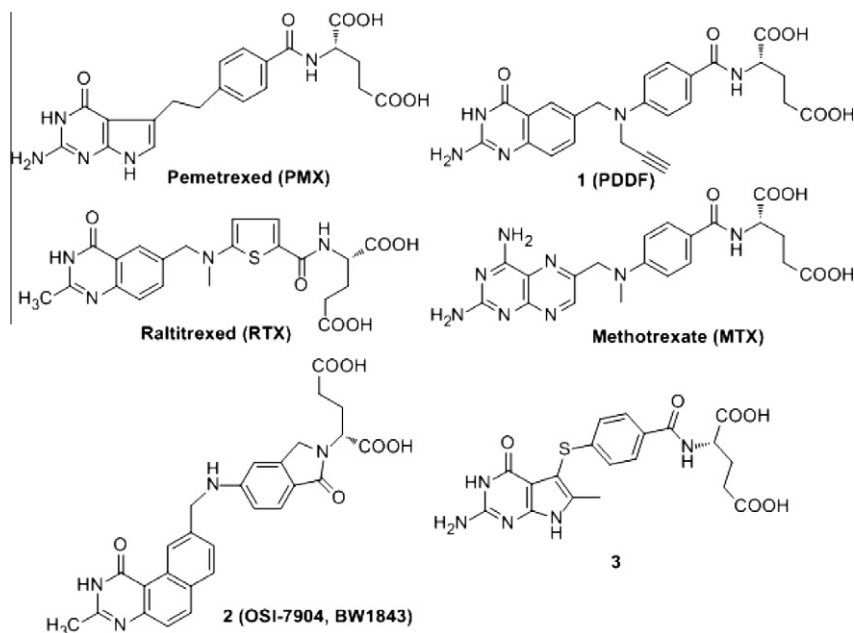


Figure 1. Antifolates.

It has been our long-standing goal not only to design potent TS and DHFR inhibitors but also to design and synthesize single agents that have potent dual TS and DHFR inhibitory activity simultaneously. Such dual inhibitors could act at two different sites (TS and DHFR) and might be capable of providing 'combination chemotherapy' in single agents without the pharmacokinetic, overlapping toxicities and other disadvantages of two separate agents.²⁰ This strategy may also lead to an improved toxicity profile.

Typically, antifolates that contain a 2-methyl-4-oxo substitution in the pyrimidine ring (such as RTX) are TS inhibitors, while 2-amino-4-oxo substitution in the pyrimidine ring (such as PMX) may provide affinity for both TS and DHFR. 2,4-Diamino substitutions on the pyrimidine ring of antifolates is usually associated with DHFR inhibitory activity.

In an attempt to prevent or minimize the potential problems associated with FPGS, including tumor resistance, and to develop dual TS and DHFR inhibitors, Gangjee et al.²⁰ reported the synthesis of a classical antifolate *N*-{4-[(2-amino-6-methyl-4-oxo-4,7-dihydro-3*H*-pyrrolo[2,3-*d*]pyrimidin-5-yl)thio]benzoyl}-L-glutamic acid, **3** (Fig. 1), as a potent inhibitor of isolated hTS ($IC_{50} = 42$ nM) with a reasonable inhibition of human recombinant DHFR ($IC_{50} = 2.2$ μ M) in its monoglutamate form thus providing dual inhibitory activity of TS and DHFR. Compound **3** was equipotent with **1** (Fig. 1), a potent TS inhibitor, against hTS and was more potent than the clinically used RTX and PMX against isolated hTS in their monoglutamate forms. Molecular modeling (SYBYL 6.91)²² suggested that the 6-methyl group in compound **3** makes important hydrophobic contacts with Trp109 in hTS and also serves to lock the 5-position side chain into favorable, low energy conformations. Both these factors probably contribute to the high inhibitory activity of **3** in its monoglutamate form against hTS.

A potential advantage of compound **3** over RTX and PMX is that it is not a substrate for hFPGS, from CCRF-CEM cells, at concentrations up to 1045 μ M.²⁰ The lack of hFPGS substrate activity of **3** was attributed, in part, to the presence of the 6-methyl group on the pyrrolo[2,3-*d*]pyrimidine of **3**. The 6-methyl group of **3** probably creates steric hindrance in its binding to the active site of hFPGS. Alternatively, the 6-methyl group of **3** may force the 5-position side chain into a conformation, that is, not conducive

for binding to hFPGS. The fact that PMX, a pyrrolo[2,3-*d*]pyrimidine, much like **3**, lacks a 6-methyl group and is a substrate for FPGS lends credence to the involvement of the 6-methyl moiety in preventing FPGS substrate activity in **3**.

Tricyclic **2** (Fig. 1) is a classical TS inhibitor with $K_i = 0.09$ nM.^{23,24} Although this compound is an excellent substrate for FPGS, it is subject to the addition of only one additional glutamic acid. Moreover, the high potency of **2** does not rely on polyglutamation as the monoglutamate form is equi-potent with the diglutamate form.²⁵ Compound **2** is a noncompetitive TS inhibitor and its activity is not affected by the concentration of 5,10-CH₂THF.^{23,24} In addition, it has been demonstrated that overexpression of the multidrug resistance proteins, MRP1 and MRP2, can confer tumor resistance to short term (4 h), but not long term (72 h), exposure of **2**.²⁶

In the course of our structure-based drug design program it was of interest to synthesize classical antifolates **4–7** with a tricyclic benzo[4,5]thieno[2,3-*d*]pyrimidine scaffold (Fig. 2), as structural hybrids of **2** and **3**. Compounds **4** and **5**, similar to **2**, have a 2-methyl-4-oxo pyrimidine ring which is generally associated with TS inhibition. In contrast, **6** and **7** have a 2-amino-4-oxo substitution, which could afford dual TS and DHFR inhibition, as observed for **3** and PMX. The 2-substitutions on **4–7** would assess the

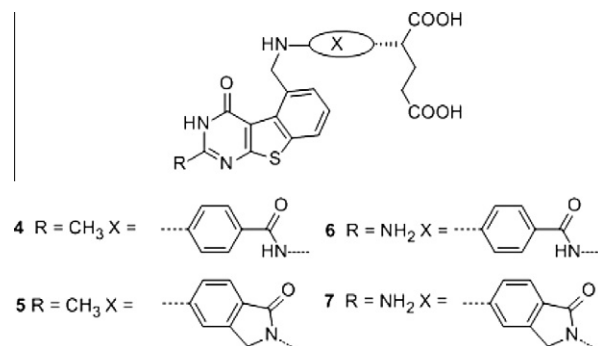


Figure 2. Target classical antifolates with the tricyclic benzo[4,5]thieno[2,3-*d*]pyrimidine scaffold.

importance of hydrogen-bonding at this position (**6**, **7**) versus hydrophobic binding (**4**, **5**) to biological activity. The size of a sulfur atom in **4–7** is larger than a nitrogen atom and smaller than two carbon atoms, thus the thiophene B-ring in benzo[4,5]thieno[2,3-*d*]pyrimidines **4–7** mimics both the smaller pyrrolo B-ring in **3** and the larger quinazoline B-ring in **2** (Fig. 3).

Similar to the C-ring in **2** and the 6-methyl group in **3**, the benzo C-ring in **4–7** makes hydrophobic contacts with Trp109 in hTS and restricts the side chain to a conformation conducive for potent TS activity but perhaps not for FPGS substrate activity.

To explore the effects of side chain flexibility on biological activity, **4** and **6** have the same benzoylglutamate side chain as **3**, while **5** and **7** have a more conformationally restricted 2-isoindolinylglutamate side chain like **2**. Unlike other classical TS inhibitors, the glutamate side chain in **2** is part of an isoindolinone system, which restricts the side chain conformation. The crystal structure of ternary complex TS-dUMP-**2** (PDB: 1SYN)²⁷ revealed that the binding of **2** and the nucleotide induced a closed conformation of the TS protein, similar to other antifolates. Surprisingly, however, the binding surface of **2** includes a hydrophobic patch from Val 77, that is, normally buried.^{27–30}

As shown in Figure 4, molecular modeling using MOE 2008.10³¹ revealed that when the central ring in **2** is truncated to a five-member ring in the benzo[4,5]thieno[2,3-*d*]pyrimidine **5**, and the substitution is moved from the 6-position to the 5-position, the resulting compound could bind to TS in a manner similar to **2**.

2. Chemistry

It was envisioned that target compounds **4–7** would be synthesized via the coupling between the benzo[4,5]thieno[2,3-*d*]pyrimidine scaffold and the glutamate side chain.

The synthesis of benzo[4,5]thieno[2,3-*d*]pyrimidines started from commercially available α -methyl cyclohexanone (\pm)-**8** to the thiophene intermediate (\pm)-**9** (Scheme 1) via a Gewald reaction³² in 81% yield. The reaction was attempted in various solvents and bases with the optimized results obtained with ethanol and morpholine. Cyclization of (\pm)-**9** via the partially aromatized tricyclic intermediate should afford benzo[4,5]thieno[2,3-*d*]pyrimidines. To explore this strategy, (\pm)-**10** (Scheme 1) was synthesized via the condensation of (\pm)-**9** and chloroformamide hydrochloride.³³ Aromatization of (\pm)-**10** was expected to afford **12** (Scheme 1).

Rosowsky et al.³⁴ reported aromatization of tetracyclic thieno[2,3-*d*]pyrimidine via SeO₂ in acetic acid at reflux. Attempts at this reaction for the conversion of (\pm)-**10** to **12** were unsuccessful. Gangjee et al.³⁵ reported the oxidation of dihydropyrrolo[2,3-*d*]pyrimidines to their aromatic congeners via MnO₂ oxidation. However, MnO₂ oxidation for the aromatization of (\pm)-**10** was also unsuccessful. DDQ is reported³⁶ to serve as a dehydrogenation

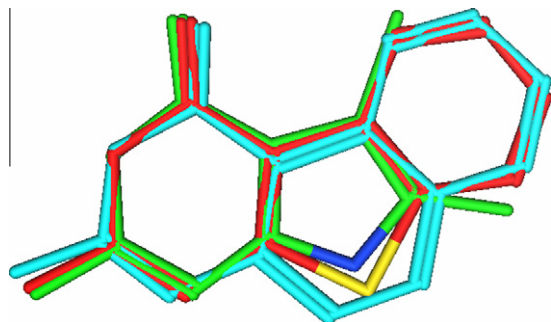


Figure 3. Superimposition of benzo[4,5]thieno[2,3-*d*]pyrimidine (red), pyrrolo[2,3-*d*]pyrimidine (green) and benzo[4,5]quinazoline (cyan).

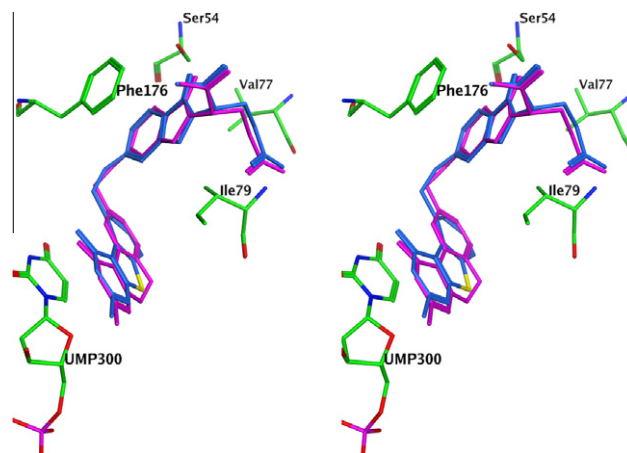
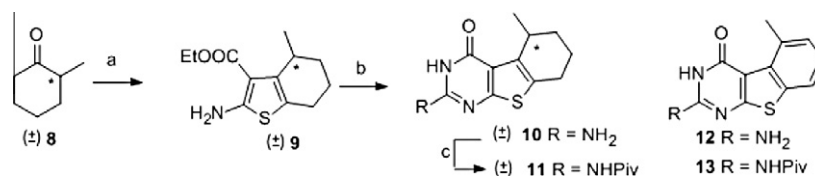


Figure 4. Stereoview of compound **5** (blue) superimposed on **2** (purple) in eTS (green). Figure prepared with MOE 2008.10.³¹

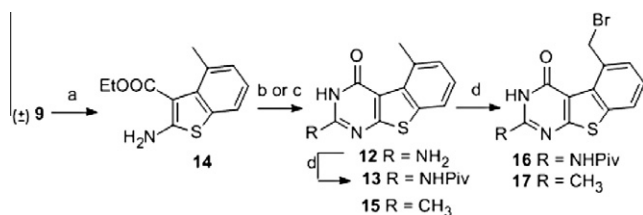
agent to effect aromatization. Reaction of (\pm)-**10** with DDQ at reflux in dioxane for up to 24 h afforded no new product (TLC). Other solvents with different boiling points were also attempted at reflux and microwave conditions. Trace amounts of a new product was observed under certain conditions, however, the yields were poor and precluded characterization.

The poor solubility of (\pm)-**10** in organic solvents could, in part, be responsible for the failure of aromatization. Thus, the 2-amino group in (\pm)-**10** was protected with a pivaloyl group at reflux with the anhydride (Piv)₂O (Scheme 1) to give (\pm)-**11**, which was then subjected to DDQ oxidation under different reaction conditions. Unfortunately, no desired product was obtained.

The failure of the previous strategy prompted us to explore an alternate method, where the bicyclic scaffold was aromatized first (Scheme 2). Bicyclic intermediate (\pm)-**9** showed good solubility in most organic solvents. With toluene as the solvent and MnO₂, SeO₂ or DDQ as the oxidant, under bench-top conditions or microwave irradiation no desired product was obtained. A literature search revealed Pd/C oxidation.^{37,38} This allowed the conversion of (\pm)-**9** to the fully aromatized **14**. The solvent and time of the reaction were optimized for the aromatization with the optimal conditions being mesitylene as solvent at reflux for 48 h. Compared with (\pm)-**9**, the ¹H NMR of **14** showed the disappearance of protons at δ 1.54–3.17 ppm and the appearance of three aromatic protons at δ 6.98–7.43 ppm, which confirmed aromatization. In addition, the appearance of benzylic protons at δ 2.38 as singlet also confirmed aromatization. With **14** in hand, cyclization was carried out to afford the tricyclic scaffold. The substitution at the 2-position of the benzo[4,5]thieno[2,3-*d*]pyrimidine are predicated by the reactant. Cyclization of **14** (Scheme 2) with chloroformamide hydrochloride afforded the 2-amino-4-oxo benzo[4,5]thieno[2,3-*d*]pyrimidine **12** in 60% yield. Pivaloylation of **12** afforded **13**. The reaction of **14** in acetonitrile with gaseous hydrogen chloride afforded the 2-methyl-4-oxo product **15** in 57% yield. The 2-methyl and 5-methyl groups of **15** occur in the ¹H NMR at δ 2.35 and 2.95, respectively, akin to similar dimethyl substituted quinazolines and benzoquinazolines.^{39,23,40,41} Free radical bromination of **13** and **15** with *N*-bromosuccinimide and a catalytic amount of benzoyl peroxide afforded intermediates **16** and **17** respectively.^{39,23,40} By limiting the amount of the NBS to just over 1 equiv, the 5-methyl moiety of **15** was selectively brominated to afford **17**, similar to that reported for quinazolines and benzoquinazolines.^{39,23,40,41} The 2-methyl moiety of **17** occurs in the ¹H NMR at δ 2.69 and the 5-methylene protons occur at δ 5.84 similar to the corresponding quinazolines and benzoquinazolines.^{39,23,40,41}



Scheme 1. Synthesis of tricyclic thieno[2,3-*d*]pyrimidines **10** and **11**. Reagents and conditions: (a) ethylcyanoacetate, morpholine, sulfur, ethanol, 45 °C to rt, 12 h; (b) chloroformamidinium hydrochloride, DMSO₂, 150 °C; (c) (Piv)₂O, reflux, 3 h.



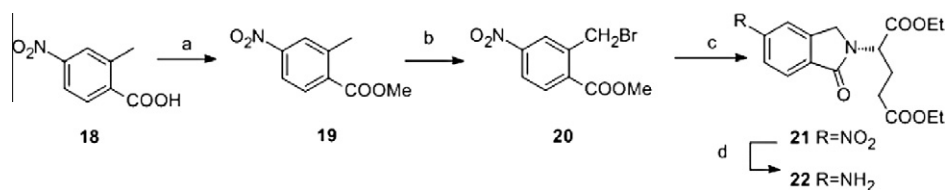
Scheme 2. Synthesis of tricyclic thieno[2,3-*d*]pyrimidines **16** and **17**. Reagents and conditions: (a) Pd/C, toluene, reflux; (b) HCl (g), acetonitrile, ammonium hydroxide; (c) chloroformamidinium hydrochloride, DMSO₂, 150 °C; (d) (Piv)₂O, reflux, 3 h, NBS, Bz₂O₂.

The benzoylglutamate side chain for **4** and **6** is commercially available, however the 2-isoindolinynglutamate side chain for **5** and **7** was synthesized via a literature method (Scheme 3).³⁹ Esterification of **18** with SOCl₂ in methanol afforded **19** in 91% yield. Radical bromination of **19** with *N*-bromosuccinimide and a catalytic amount of benzoyl peroxide afforded **20** in 48% yield. The ¹H NMR of **20** showed the disappearance of protons at δ 2.69 ppm (CH₃) and appearance of protons at δ 4.86 ppm (CH₂Br). Treatment of **20** with excess diethyl *L*-glutamate hydrochloride and K₂CO₃ in DMF at room temperature afforded isoindolone **21** as an orange oil in 56% yield. The ¹H NMR of **21** showed the appearance of protons at δ 4.51–4.83 ppm (isoindolone CH₂) and δ 5.09–5.14 ppm (Glu-CH). Reduction of the nitro group in **21** afforded the amine **22** in 92.5% yield.

As shown in Scheme 4, *N*-alkylation⁴² of **16** and **17** followed by hydrolysis of the ethyl ester (and the removal of pivaloyl protecting group in **6–7**) with 1 N NaOH and subsequent acid workup afforded target compounds **4–7**. The presence of glutamate in the side chain was confirmed from ¹H NMR. The expected NH at δ 6.74–7.40 ppm, exchanged with D₂O, and the benzylic protons occurred as a doublet at δ 5.13–5.24 ppm, which converts to a singlet upon D₂O exchange, indicated the success of the coupling reaction. High resolution MS (HRMS) and the presence of the requisite protons of the side chain via NMR confirmed the structure of **4–7**.

3. Biological evaluation and discussion

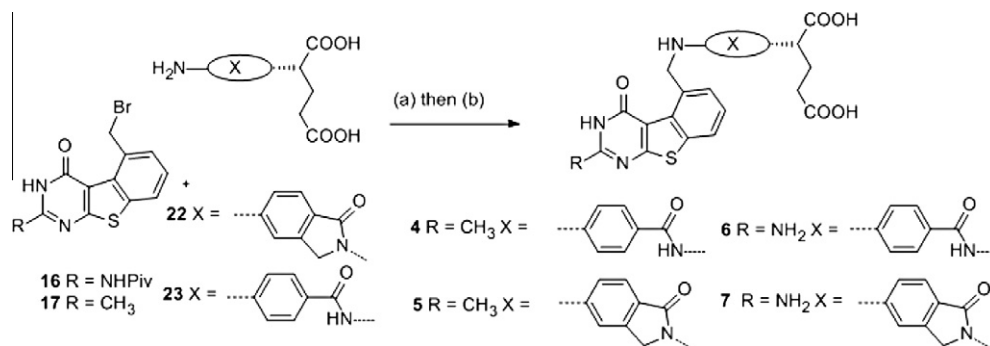
Compounds **4–7** were evaluated as inhibitors of TS and DHFR (Table 1) from three different sources; human, *Escherichia coli* and *Toxoplasma gondii*. Compound **1** (PDDF) was used as the standard compound for TS inhibition and MTX was used as the standard compound for DHFR inhibition. For comparison, the



Scheme 3. Synthesis of side-chain **22**. Reagents and conditions: (a) SOCl₂, MeOH; (b) NBS, Bz₂O₂; (c) diethyl glutamate (d) H₂, Pd/C.

activities of PMX and lead compounds **2** and **3** are also provided. The classical benzo[4,5]thieno[2,3-*d*]pyrimidines **6–7** showed potent hTS inhibitory activity comparable to that of **1**, **2** and **3** which supports the hypothesis that a 6-5-6 tricyclic system with a 5-substitution can inhibit TS in a similar fashion as the 6-6-6 tricyclic system with a 6-substitution. Compound **7** is the most potent hTS inhibitor in the series and is two-fold more potent than compound **1** and equipotent with compound **2**. Against isolated hTS, all four compounds **4–7** showed 50 to 100-fold greater activity than PMX, which relies on FPGS for its potent hTS inhibitory activity. Thus compounds **4–7**, and in particular **6** and **7**, have the potential to overcome the tumor resistance problems of PMX associated with lower levels of FPGS. With identical side chain substitution, the 2-amino analogs are more potent than the 2-methyl compounds. This indicates the importance of hydrogen bonding ability at the 2-position. Side chain flexibility could also play a role in enzyme inhibition. When the 2-substitution is methyl, the more rigid side chain analog **5** is three-fold less potent than the more flexible **4** against hTS. However, this trend is reversed when the 2-substitution is an amino group, where the more rigid compound **7** is twice as potent as the flexible **6**. These data suggest that the conformation of side chain glutamate along with the 2-substitution pattern dictates enzyme binding.

Compounds **4** and **5** are inactive against DHFR from different sources, while **6** and **7** are about equally potent against hDHFR and are about five-times less potent than MTX. Compounds **6** and **7** also have different selectivity profile than MTX. MTX is three-times more selective for *E. coli* (ec) DHFR than hDHFR, while **6** and **7** are more selective for hDHFR and the selectivity index is about 4. Inhibition of DHFR by **6** and **7** confirms our hypothesis that the replacement of the 2-methyl group by 2-amino group in benzo[4,5]thieno[2,3-*d*]pyrimidines can provide dual TS and DHFR inhibition. The inactivity of **4** and **5** against hDHFR is probably due to the absence of a salt bridge with Glu30 of hDHFR at the N1 and 2NH₂. While compounds **6** and **7** can bind just like folate (PDB: 1U72) in which the 2-amino-4-oxo group binds to the enzyme with hydrogen bonding and the heterocycle and the benzoyl moieties bind to Phe31, Phe34 and Ile 60. The α-carboxylic acid of the glutamate makes ionic contact with Arg70. A second mode of binding would involve a 180° rotation about the C-2, NH₂ bond (Fig. 5), whereby the sulfur of the thiophene ring is now superimposed on the 4-oxo group of folate, with all other interactions being the same. It is important to note that binding of **6** and **7** in the flip mode (Fig. 5) also allows the sulfur of the thiophene ring to mimic the 4-amino of MTX. To determine which of these two modes of



Scheme 4. Synthesis of classical analogs **4–7**. Reagents and conditions: (a) DMF, reflux; (b) 1 N NaOH 60 °C.

Table 1
Inhibitory concentrations (IC_{50} in ΦM) Against TS and DHFR^a

Compound	TS (μM)			DHFR (μM)		
	Human ^b	<i>E. coli</i> ^b	<i>T. gondii</i> ^c	Human ^d	<i>E. coli</i> ^e	<i>T. gondii</i> ^c
1 ^f	0.064	0.048	0.072	11	11	0.26
2 ^g	0.032	0.023	0.027	>20 (16)	20	0.71
3 ^h	0.053	0.21	0.09	2.1	22	0.23
4	0.26	0.82	1.7	>20 (35)	15	1.4
5	0.8	0.85	3.7	>20 (24)	>20 (38)	1.8
6	0.068	0.017	0.14	0.09	0.4	0.02
7	0.034	0.05	0.17	0.1	0.4	0.01
PMX ^h	9.5	76	2.8	6.6	2300	0.43
MTX	>18 (29)	>18 (14)	>18 (36)	0.022	0.0044	0.022

^a The percent inhibition was determined at a minimum of four inhibitor concentrations within 20% of the 50% point. The standard deviations for determination of 50% points were within $\pm 10\%$ of the value given.

^b Kindly provided by Dr. Frank Maley, New York State Department of Health.

^c Kindly provided by Dr. Karen Anderson, Yale University, New Haven, CT.

^d Kindly provided by Dr. J.H. Freisheim, Medical College of Ohio, Toledo, OH.

^e Kindly provided by Dr. R.L. Blakley, St. Jude Children's hospital, Memphis, TN.

^f Kindly provided by Dr. M.G. Nair, University of South Alabama.

^g Kindly provided by Dr. J.J. McGuire, Roswell Park Cancer Institute, Buffalo, NY.

^h Kindly provided by Dr. Chuan Shih, Eli Lilly and Co.

binding the molecule adopts to bind hDHFR, **6** and **7** were each cocrystallized with isolated hDHFR.

4. X-ray crystal structures

The X-ray crystal structures of the ternary complexes of tricyclic compounds **6** and **7** and NADPH with hDHFR were determined and refined to 1.35 Å resolution. These data show, for the first time, that the tricyclic benzo[4,5]thieno[2,3-*d*]pyrimidine antifolates **6** and **7** bind in a folate orientation such that the 2-NH₂ and N3 interact with Glu30 and the thienosulfur occupies the N8 position observed in the binding of folic acid (Figs. 6 and 7). These results

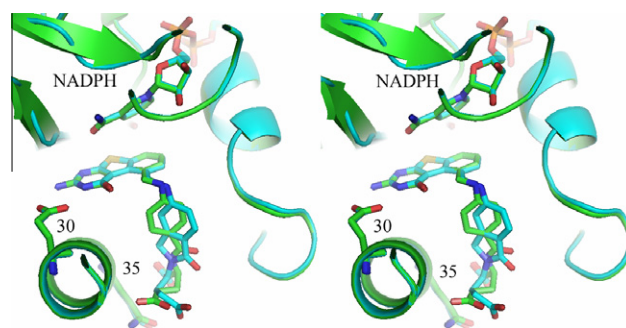


Figure 6. Stereoview of the X-ray crystal structures of **6** (green) and **7** (cyan) superimposed in the active site of hDHFR and NADPH ternary complex..

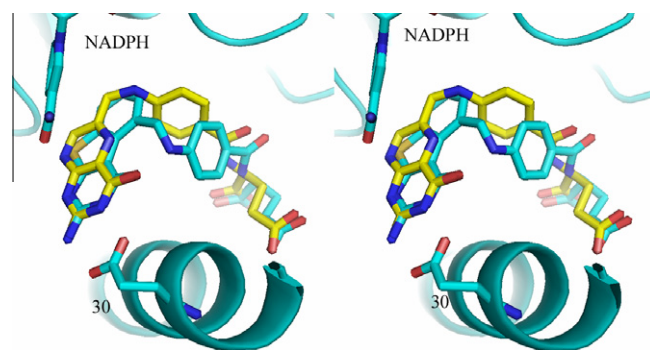


Figure 7. Stereo comparison of the structure of **6** (cyan) with that of folate (yellow) in hDHFR. Figure prepared with PyMol.⁴⁵

are similar to those observed for the bicyclic structure of the *N*-{4-[2-amino-6-methyl-4-oxo-3,4-dihydrothieno[2,3-*d*]pyrimidin-5-yl]thio]benzoyl}-*L*-glutamic acid⁴³ in complex with active site mutants of hDHFR in which the thieno[2,3-*d*]pyrimidine ring sulfur in both complexes makes intermolecular contacts with the

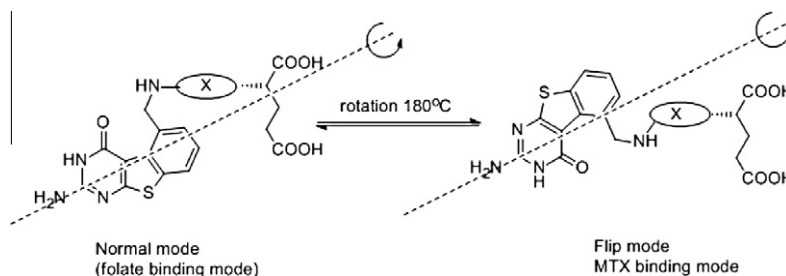


Figure 5. Proposed binding mode with DHFR.

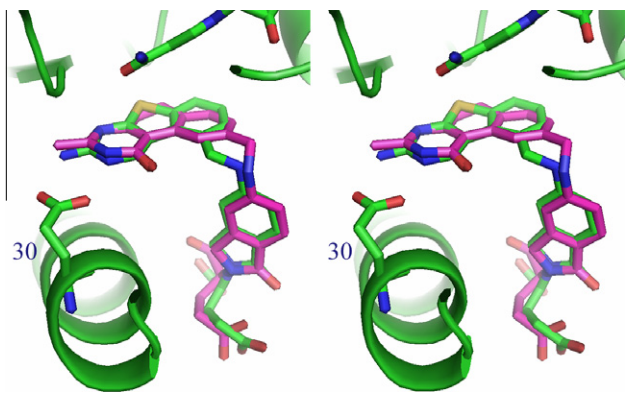


Figure 8. Model of **2** (violet) from ecTS²⁸ structure modeled to **7** in hDHFR (green).

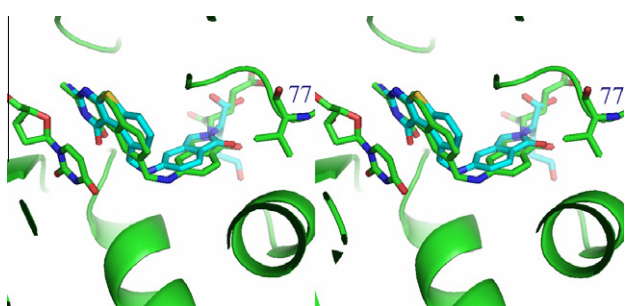


Figure 9. Stereoview of ecTS-2²⁸ (green) with compound **7** (cyan) from the crystal structure of hDHFR fit to the TS ligand. Also highlighted is residue Val77 in TS.

carbonyl of Ile7 (3.5 Å), Val115 (3.7 Å), the hydroxyl of Tyr121 (3.8 Å) and the carbonyl of the nicotinamide ring (3.6 Å). Thus the steric addition of the benzo fused ring does not prevent the thieno S from making the same contacts with hDHFR as that of the 4-NH₂ of MTX.⁴⁴

Although molecular modeling studies suggest that both a flipped and folate orientation were possible for these structures (Fig. 5), the observed crystal structures reveal, for the first time, only binding in the normal mode of folate orientation, as illustrated in Figure 7 that compares the binding of **6** with folate. The binding orientation of the 6-5-6-ring system is the same in **6** and **7** while the added ring in the isoindoline ring system of **7** shows, also for the first time, that the fused isoindolinyl ring system side chain of **7** is flipped compared to that of the normal *p*-aminobenzoylglutamate of **6** as illustrated in Figure 6. Despite this change, the functional groups of the L-glutamate side chain still occupy similar positions in the binding site. To our knowledge this is the first time that the fused conformationally restricted isoindolinyl ring system side chain has been compared side-by-side in a X-ray structure with the benzoyl ring in hDHFR.

Comparison of binding of **2** from the structure of ecTS²⁸ modeled into the binding site of **7** in hDHFR (from the X-ray crystal structure) shows that there are changes in the *p*-aminobenzoyl bridge conformation (Fig. 8) that result from the displacement of the 6-6-6-ring system of **2** compared to the 6-5-6-ring system of **7**. Similarly, a fit of **7** to that of **2** in ecTS (Fig. 9) shows that contact with Val 77 is the same for both **7** and **2** (Fig. 9).

5. Conclusion

Compounds **4–7** were synthesized as classical antifolates with both rigid and flexible benzoylglutamates attached to the tricyclic benzo[4,5]thieno[2,3-*d*]pyrimidine scaffold. Compounds with a 2-CH₃ moiety inhibited human TS but not human DHFR.

Replacement of the 2-CH₃ moiety with a 2-NH₂ gave increased human TS inhibition and also human DHFR inhibition affording dual hTS/hDFHR inhibitors. The X-ray crystal structures of **6** and **7** show, for the first time, that tricyclics **6** and **7** bind in the folate rather than the MTX mode.

6. Experimental section

All evaporations were carried out in vacuo with a rotary evaporator. Analytical samples were dried in vacuo (0.2 mmHg) in a CHEM-DRY drying apparatus over P₂O₅ at 80 °C. Melting points were determined on a MEL-TEMP II melting point apparatus with a FLUKE 51 K/J electronic thermometer and are uncorrected. Nuclear magnetic resonance spectra for proton (¹H NMR) were recorded on either a Bruker WH-400 (400 MHz) spectrometer or a Bruker WH-300 (300 MHz) spectrometer. The chemical shift values are expressed in ppm (parts per million) relative to tetramethylsilane as an internal standard: s, singlet; d, doublet; t, triplet; q, quartet; m, multiplet; br, broad singlet; exch, D₂O exchangeable protons. Mass spectra were recorded on a VG-7070 double-focusing mass spectrometer or in a LKB-9000 instrument in the electron ionization (EI) mode. Chemical names follow IUPAC nomenclature. Thin-layer chromatography (TLC) was performed on Whatman Sil G/UV254 silica gel plates with a fluorescent indicator, and the spots were visualized under 254 and 365 nm illumination. All analytical samples were homogeneous on TLC in three different solvent systems. Proportions of solvents used for TLC are by volume. Column chromatography was performed on a 230–400 mesh silica gel (Fisher, Somerville, NJ) column. Elemental analyses were performed by Atlantic Microlab, Inc., Norcross, GA. Element compositions are within 0.4% of the calculated values. Fractional moles of water frequently found in the analytical sample of antifolates could not be prevented in spite of 24–48 h of drying in vacuo and was confirmed where possible by the presence in the ¹H NMR spectra. All solvents and chemicals were purchased from Aldrich Chemical Co. or Fisher Scientific and were used as received. For compounds **4–7**, a single spot on TLC in three different solvent systems with three different R_f values confirmed >95% purity.

6.1. Ethyl 2-amino-4-methyl-4,5,6,7-tetrahydro-1-benzothiothiophene-3-carboxylate (**9**)

A mixture of sulfur (1.1 g, 36 mmol), 2-methylcyclohexanone (4.04 g, 36 mmol), ethyl cyanoacetate (4.07 g, 36 mmol) and EtOH (150 mL) were placed in a round bottom flask and warmed to 45 °C and treated dropwise with morpholine (3.1 g, 36 mmol) over 15 min. The mixture was stirred for 5 h at 45 °C and 24 h at room temperature. Unreacted sulfur was removed by filtration, and the filtrate was concentrated under reduced pressure to afford an orange solid. The residue was loaded on a silica gel column packed with silica gel and eluted with 10% ethyl acetate in hexane. The fractions containing the desired product (TLC) were pooled and evaporated to afford **9** (6.97 g, 80.9%) as an orange solid; mp 69.9–71 °C; R_f 0.44 (hexane/EtOAc 3:1); ¹H NMR (DMSO-*d*₆): δ 1.08–1.10 (d, 3H, *J* = 6.6 Hz, 4-CH₃), 1.25–1.28 (t, 3H, *J* = 6.8 Hz, COOCH₂CH₃), 1.57–1.78 (m, 4H), 2.39–2.43 (m, 2H), 3.15–3.17 (m, 1H), 4.10–4.24 (q, 2H, *J* = 6.8 Hz, COOCH₂CH₃), 7.23 (s, 2H, NH₂ exch). Titled compound was used directly for next step without further characterization.

6.2. 2-Amino-5-methyl-5,6,7,8-tetrahydro[1]benzothieno[2,3-*d*]pyrimidin-4(3H)-one (**10**)

A mixture of **9** (0.74 g, 3.28 mmol) and chloroformamide hydrochloride (1.51 g, 13.12 mmol) in dimethyl sulfoxide (DMSO₂)

(4 g) was heated at 140 °C for 4 h. The mixture was cooled to room temperature and water (15 mL) was added and ammonium hydroxide was used to neutralize the suspension. The brown solid, obtained by filtration, was washed with water and dried over P₂O₅ in vacuum. The solid was dissolved in methanol and silica gel was added. A dry silica gel plug was obtained after evaporation of the solvent. The plug was loaded on to a silica gel column and eluted with 5% methanol in chloroform. The fractions containing the desired product (TLC) were pooled and evaporated to afford **10** (0.46 g, 59.7%) as a light yellow solid; mp >300 °C; R_f 0.5 (MeOH/CHCl₃, 1:6); ¹H NMR (DMSO-*d*₆) δ 1.18–1.20 (d, 3H, *J* = 6.8 Hz, CH₃), 1.59–1.61 (m, 1H), 1.71–1.83 (m, 3H), 2.54–2.64 (m, 2H), 3.15–3.18 (m, 1H), 6.39 (s, 2H, 2-NH₂ exch), 10.73 (s, 1H, 3-NH exch); Anal. (C₁₁H₁₃N₃SO·0.2H₂O): C, H, N, S.

6.3. 2,2-Dimethyl-N-(5-methyl-4-oxo-3,4,5,6,7,8-hexahydro[1]benzothieno[2,3-*d*]pyrimidin-2-yl)propanamide (11)

To a 100 mL round-bottomed flask was added **10** (0.706 g, 3 mmol) and excess Piv₂O (10 mL). The mixture was kept at reflux for 2 h. The excess Piv₂O was removed under vacuum and the residue was made into silica gel plug. The silica gel plug obtained was loaded onto a silica gel column and eluted with 1:8 ethyl acetate/hexane. The fraction containing the desired product were pooled afford **11** (0.956 g, 70.3%) as a white solid; mp 236.6–237.8 °C; R_f 0.31 (hexane/EtOAc 3:1); ¹H NMR (DMSO-*d*₆) δ 1.22 (s, 12H, 4 CH₃), 1.62–1.79 (m, 4H), 2.58–2.73 (m, 2H), 3.23 (br s, 1H), 11.07 (s, 1H, NH exch), 12.02 (s, 1H, NH exch). Titled compound was used directly for next step without further characterization.

6.4. Ethyl 2-amino-4-methyl-1-benzothiophene-3-carboxylate (14)

A mixture of **9** (0.239 g, 1 mmol), 10% Pd/C (0.239 g) and mesitylene (50 mL) were placed in a round bottom flask and kept at reflux for 1–2 days. The mixture was cooled to room temperature and Pd/C was removed by filtration, and the filtrate was concentrated under reduced pressure to afford a brown oil. The residue was loaded on a silica gel column and eluted with 10% ethyl acetate in hexane. The fractions containing the desired product (TLC) were pooled and evaporated to afford **14** (0.123 g, 52.1%) as an orange semi solid; R_f 0.38 (hexane/EtOAc 3:1); ¹H NMR (DMSO-*d*₆): δ 1.29–1.32 (t, 3H, *J* = 6.8 Hz, COOCH₂CH₃), 2.38 (s, 3H, CH₃), 4.25–4.30 (q, 2H, *J* = 6.8 Hz, COOCH₂CH₃), 6.98–7.04 (m, 2H, C₆H₃), 7.44, 7.45 (d, 1H, *J* = 4 Hz, C₆H₃), 7.43 (s, 2H, NH₂ exch). Titled compound was used directly for next step without further characterization.

6.5. 2-Amino-5-methyl[1]benzothieno[2,3-*d*]pyrimidin-4(3H)-one (12)

A mixture of **14** (0.49 g, 2.07 mmol) and chloroformamide hydrochloride (1.19 g, 10.37 mmol) in DMSO₂ (2 g) was heated at 140 °C for 2 h. The mixture was cooled to room temperature and water (15 mL) was added and ammonium hydroxide was used to neutralize the suspension. The brown solid, obtained by filtration, was washed with water and dried over P₂O₅ vacuum. The solid was dissolved in methanol and silica gel (1.0 g) was added. A dry silica gel plug was obtained after evaporation of the solvent. The plug was loaded on to a silica gel column and eluted with 5% methanol in chloroform. The fractions containing the desired product (TLC) were pooled and evaporated to afford **12** (0.29 g, 60.7%) as a yellow solid; mp >300 °C; R_f 0.41 (MeOH/CHCl₃, 1:6); ¹H NMR (DMSO-*d*₆) δ 2.87 (s, 3H, CH₃), 6.82 (s, 2H, 2-NH₂ exch), 7.13–7.17 (m, 2H, C₆H₃), 7.57, 7.59 (d, 1H, *J* = 8.0 Hz, C₆H₃), 10.92 (s, 1H, 3-NH exch).

Titled compound was used directly for next step without further characterization.

6.6. 2,2-Dimethyl-N-(5-methyl-4-oxo-3,4-dihydro[1]benzothieno[2,3-*d*]pyrimidin-2-yl)propanamide (13)

To a 100 mL round-bottomed flask was added **12** (1.34 g, 5.8 mmol) and excess Piv₂O (4 equiv). The mixture was kept at reflux for 2 h. The excess Piv₂O was removed under vacuum and the residue was made into silica gel plug. The silica gel plug obtained was loaded onto a silica gel column and eluted with 1:8 ethyl acetate/hexane to afford **13** (1.299 g, 70.9%) as a white solid, mp 178.3–179.5 °C; R_f 0.35 (hexane/EtOAc 3:1); ¹H NMR (CDCl₃) δ 1.35 (s, 9H, 3 CH₃ of Piv), 3.05 (s, 3H, CH₃), 7.28 (m, 2H, C₆H₃), 7.56, 7.59 (d, 1H, *J* = 8.0 Hz C₆H₃), 8.14 (s, 1H, NH exch), 11.86 (s, 1H, NH exch). Titled compound was used directly for next step without further characterization.

6.7. 2,5-Dimethyl[1]benzothieno[2,3-*d*]pyrimidin-4(3H)-one (15)

To a 100 mL round flask were added **14** (2.35 g, 10 mmol) and CH₃CN (50 mL). Vigorous stirring afforded, a clear solution. Anhydrous HCl gas was bubbled into the solution for 1 h to give a thick precipitate, which then redissolved into the acid solution. Anhydrous HCl gas was added for an additional 3 h after which the reaction mixture became clear. Evaporation of the solvent under reduced pressure afforded a residue that was dissolved in water. Concentrated aqueous NH₄OH was added to afford a suspension at pH 8. The precipitate was collected by filtration, washed with water and dried over P₂O₅ in a vacuum to afford **15** (1.0 g, 57%) as a yellow solid; mp >300 °C; R_f 0.58 (MeOH/CHCl₃, 1:6); ¹H NMR (DMSO-*d*₆) δ 2.35 (s, 3H, 2-CH₃), 2.95 (s, 3H, 5-CH₃), 7.29 (m, 2H, C₆H₃), 7.78 (s, 1H, C₆H₃), 12.54 (s, 1H, 3-NH exch). HRMS calcd for C₁₂H₁₀N₂O₂S 231.0592, found 231.0584.

6.8. 5-(Bromomethyl)-2-methyl[1]benzothieno[2,3-*d*]pyrimidin-4(3H)-one (17)

To a 100 mL flask were added **15** (0.736 g, 3.2 mmol) and benzene (30 mL). The suspension was stirred at 60 °C for 30 min to afford a clear solution, followed by the addition of *N*-bromosuccinimide (0.620 g, 3.49 mmol) and benzoyl peroxide (50 mg). The mixture was maintained at reflux for 4 h and then cooled to room temperature and washed with water, and evaporated to afford a yellow solid. The solid was dissolved in methanol and silica gel (1.5 g) was added. A dry silica gel plug was obtained after evaporation of the solvent. The plug was loaded on to a silica gel column and eluted with 6% ethyl acetate in hexane to afford **17** (393 mg, 39%) as a white solid; mp 217.8–219.1 °C; R_f 0.3 (hexane/EtOAc 3:1); ¹H NMR (CDCl₃) δ 2.69 (s, 3H, 2-CH₃), 5.84 (s, 2H, CH₂Br), 7.44–7.47 (t, 1H, *J* = 7.2, C₆H₃), 7.57–7.58 (d, 1H, *J* = 7.2 Hz, C₆H₃), 7.80–7.82 (d, 1H, *J* = 7.2 Hz, C₆H₃). HRMS calcd for C₁₂H₉N₂OSBr 307.9619, found 307.9613.

6.9. 2,2-Dimethyl-N-(5-methyl-4-oxo-3,4-dihydro[1]benzothieno[2,3-*d*]pyrimidin-2-yl)propanamide (16)

A solution of **13** (1.1 g, 3.49 mmol) in 1,2-dichloroethane (50 mL) was treated with *N*-bromosuccinimide (0.62 g, 3.49 mmol) and benzoyl peroxide (50 mg), and the mixture was maintained at reflux for 1 day. The mixture was cooled to room temperature and washed with water, and evaporated to an orange solid. The solid was dissolved in methanol and silica gel (1.5 g) was added. A dry silica gel plug was obtained after evaporation of the solvent. The plug was loaded on to a silica gel column and eluted with 6% ethyl

acetate in hexane to afford **16** (0.577 g, 41.9%) as an orange solid; mp 217.8–219.1 °C; R_f 0.3 (hexane/EtOAc 3:1); $^1\text{H NMR}$ (CDCl_3) δ 1.27 (s, 9H, 3 CH_3 of Piv), 5.71 (s, 2H, CH_2Br), 7.30, 7.33 (d, 1H, C_6H_3), 7.43, 7.46 (d, 1H, $J=7.6$ Hz, C_6H_3), 7.64, 7.66 (d, 1H, $J=4$ Hz, C_6H_3), 8.07 (s, 1H, NH exch), 11.99 (s, 1H, NH exch). Titled compound was used directly for next step without further characterization.

6.10. Methyl 2-methyl-4-nitrobenzoate (**19**)

Thionyl chloride (4.3 g, 36.45 mmol) was added dropwise to a stirred solution of **18** (3 g, 16.57 mmol) in MeOH (25 mL) while maintaining the internal temperature below 12 °C. When the addition was complete the mixture was left to stand at room temperature for 12 h to result a white precipitation. The mixture was filtered and the filtrate was concentrated under reduced pressure to afford white solid. The solid was washed with hexane and ethyl ether to afford **19** (2.95 g, 91.3%); mp 153.7–154.4 °C (lit.³⁹ mp 153–154 °C); R_f 0.43 (hexane/EtOAc 3:1); $^1\text{H NMR}$ (CDCl_3) δ 2.69 (s, 3H, CH_3), 3.95 (s, 3H, COOCH_3), 8.02–8.11 (m, 3H, C_6H_3).

6.11. Methyl 2-(bromomethyl)-4-nitrobenzoate (**20**)

A solution of **19** (2.57 g, 13.19 mmol) in 1,2-dichloroethane (100 mL) was treated with *N*-bromosuccinimide (2.3 g, 13.19 mmol) and benzoyl peroxide (0.26 g), and the mixture was kept at reflux for 2 days, then cooled, washed with water, and evaporated to a yellow oil (3.52 g). The oil was dissolved in acetone and silica gel (4.0 g) was added. A dry silica gel plug was obtained after evaporation of the solvent. The plug was loaded on to a silica gel column and eluted with 10% ethyl acetate in hexane to afford **20** (1.73 g, 48.2%) as a yellow oil; R_f 0.53 (hexane/EtOAc 3:1); $^1\text{H NMR}$ (CDCl_3) δ 3.89 (s, 3H, COOCH_3), 4.86 (s, 2H, CH_2Br), 7.98–8.23 (m, 3H, C_6H_3).

6.12. Diethyl (2S)-2-(5-nitro-1-oxo-1,3-dihydro-2H-isoindol-2-yl)pentanedioate (**21**)

The oil **20** (0.85 g, 3.1 mmol) was stirred for 16 h with diethyl glutamate hydrochloride (1.54 g, 6.4 mmol) and powdered K_2CO_3 (1.7 g, 12 mmol) in DMA (3 mL) under argon. The reaction mixture was diluted with water (20 mL) and extracted with ethyl acetate (3 \times 20 mL). The combined ethyl acetate solutions were washed twice with brine, dried, and evaporated to an orange oil. The oil was dissolved in methanol and silica gel was added. A dry silica gel plug was obtained after evaporation of the solvent. The plug was loaded on to a silica gel column and eluted with 25% ethyl acetate in hexane to afford **21** (0.63 g, 55.7%) as an orange oil; R_f 0.44 (hexane/EtOAc 1:1); $^1\text{H NMR}$ (CDCl_3) δ 1.17–1.22 (t, 3H, $\text{COOCH}_2\text{CH}_3$), 1.26–1.31 (t, 3H, $\text{COOCH}_2\text{CH}_3$), 2.19–2.49 (m, 4H, $\text{CHCH}_2\text{CH}_2\text{COOEt}$), 4.02–4.23 (2q, 4H, $\text{COOCH}_2\text{CH}_3$), 4.51–4.83 (dd, 2H, $-\text{CH}_2-$), 5.09–5.14 (m, 1H, $\text{CHCH}_2\text{CH}_2\text{COOEt}$), 8.00–8.03 (d, 1H, C_6H_3), 8.36 (br s, 2H, C_6H_3).

6.13. Diethyl (2S)-2-(5-amino-1-oxo-1,3-dihydro-2H-isoindol-2-yl)pentanedioate (**22**)

To a Parr hydrogenation bottle was added **21** (0.55 g, 1.51 mmol), 10% Pd/C (0.09 g) and acetyl acetate (30 mL). Hydrogenation was carried out at 55 psi for 12 h. After filtration, the organic phase was evaporated at vacuum to afford **22** (0.467 g, 92.5%) as an orange oil; R_f 0.19 (hexane/EtOAc 1:1); $^1\text{H NMR}$ (CDCl_3) δ 1.17–1.19 (t, 3H, $\text{COOCH}_2\text{CH}_3$), 1.20–1.25 (t, 3H, $\text{COOCH}_2\text{CH}_3$), 2.20–2.51 (m, 4H, $\text{CHCH}_2\text{CH}_2\text{COOEt}$), 4.02–4.28 (m, 6H, 2 $\text{COOCH}_2\text{CH}_3$, NH₂ exch), 4.22–4.51 (dd, 2H, $-\text{CH}_2-$), 5.03–5.07 (m, 1H, $\text{CHCH}_2\text{CH}_2\text{COOEt}$), 6.69–6.73 (m, 2H, C_6H_3), 7.60, 7.63 (d, 1H, C_6H_3).

6.14. General procedure for the synthesis of compounds 4–7

A stirred solution of the tricyclic bromide **16** or **17** (0.25 mmol) in dry DMF (5 mL) was treated with the appropriate amine **22** or **23** (1 mmol) and K_2CO_3 (95 mg, 0.69 mmol). The solution was stirred for 1 h at 80 °C under argon. The cooled reaction mixture was filtered and the filtrate was evaporated to obtain an orange solid. The solid was dissolved in methanol and silica gel was added. A dry silica gel plug was obtained after evaporation of the solvent. The plug was loaded on to a silica gel column and eluted with ethyl acetate/hexane (1:1). The fractions containing the desired product (TLC) were pooled and evaporated to afford a solid, to which a combined solution of aqueous 1 N NaOH (3 mL) and methanol (12 mL) was added. The mixture was kept at reflux for 12 h. The methanol was evaporated under reduced pressure and the residue was dissolved in water (5 mL). The solution was cooled to 0 °C and carefully acidified to pH 3 with dropwise addition of 1 N HCl. The resulting suspension was left at 0 °C for 2 h and the precipitate was collected by filtration, washed with water (5 mL) and dried over P_2O_5 /vacuum at 50 °C to afford target compounds 4–7.

6.14.1. *N*-(4-[[[(2-methyl-4-oxo-3,4-dihydro[1]benzothieno[2,3-d]pyrimidin-5-yl)methyl]amino]benzoyl]-L-glutamic acid (**4**))

Using the general procedure described above with **17** and **23** afforded **4** (37 mg, 37%) as a yellow solid; mp 219.6–221.3 °C; R_f 0.28 (MeOH/EtOAc, 1:6); R_f 0.32 (MeOH/ CHCl_3 , 1:6 + 1 drop of NEt_3); R_f 0.34 (MeOH/ CHCl_3 , 1:6 + 1 drop of gl. HOAc); $^1\text{H NMR}$ ($\text{DMSO}-d_6$): δ 1.22 (s, 1H, 2- CH_3), 1.88–2.01 (m, 2H, $\text{Glu}\gamma\text{-CH}_2\text{CH}_2$), 2.29 (m, 2H, $\text{Glu}\gamma\text{-CH}_2\text{CH}_2$), 4.31 (s, 1H, $\text{Glu}\alpha\text{-CH}$), 5.20 (s, 2H, Benzylic CH_2), 6.56–6.58 (d, 2H, $J=9.0$ Hz), 7.38–7.40 (d, 1H, $J=7.5$ Hz), 7.49 (d, 2H, 2-NH₂ exch), 7.58–7.59 (d, 2H, $J=9.0$ Hz), 7.88 (d, 1H, $J=7.5$ Hz) 8.02 (s, 1H, CONH), 8.08 (d, 1H), 12.71 (s, 1H, 3-NH exch); HRMS (ESI, pos mode) m/z [$\text{M}+\text{H}^+$] calcd for $\text{C}_{24}\text{H}_{23}\text{N}_4\text{O}_6\text{S}$ 495.1338, found 495.1345.

6.14.2. (2S)-2-(5-[[[(2-methyl-4-oxo-3,4-dihydro[1]benzothieno[2,3-d]pyrimidin-5-yl)methyl]amino]-1-oxo-1,3-dihydro-2H-isoindol-2-yl]pentanedioic acid (**5**))

Using the general procedure described above with **17** and **22** afforded **5** (35 mg, 34%) as a yellow solid; mp 236.4–237.7 °C; R_f 0.29 (MeOH/EtOAc, 1:6); R_f 0.32 (MeOH/ CHCl_3 , 1:6 + 1 drop of NEt_3); R_f 0.36 (MeOH/ CHCl_3 , 1:6 + 1 drop of gl. HOAc); $^1\text{H NMR}$ ($\text{DMSO}-d_6$): δ 1.22 (s, 3H, 2- CH_3), 1.95 (m, 2H, $\text{Glu}\beta\text{-CH}_2$), 2.18 (m, 2H, $\text{Glu}\gamma\text{-CH}_2$), 4.22 (s, 2H, isoindolinylyl CH_2), 4.67–4.69 (m, 1H, $\text{Glu}\alpha\text{-CH}$), 5.21 (s, 2H, Benzylic CH_2), 6.65 (s, 1H, CH), 6.81 (s, 1H, NH exch), 7.30–7.32 (d, 1H, $J=6.0$ Hz), 7.37–7.41 (d, 1H, $J=12$ Hz), 7.49–7.51 (d, 1H, $J=6.0$ Hz), 7.88–7.90 (d, 1H, $J=6.0$ Hz), 8.03 (s, 1H), 12.76 (s, 1H, 3-NH exch), HRMS (ESI, pos mode) m/z [$\text{M}+\text{H}^+$] calcd for $\text{C}_{25}\text{H}_{23}\text{N}_4\text{O}_6\text{S}$ 507.1333, found 507.1362.

6.14.3. *N*-(4-[[[(2-Amino-4-oxo-3,4-dihydro[1]benzothieno[2,3-d]pyrimidin-5-yl)methyl]amino]benzoyl]-L-glutamic acid (**6**))

Using the general procedure described above with **16** and **23** afforded **6** (39 g, 32%) as an orange solid; mp >300 °C; R_f 0.30 (MeOH/EtOAc, 1:6); R_f 0.34 (MeOH/ CHCl_3 , 1:6 + 1 drop of NEt_3); R_f 0.34 (MeOH/ CHCl_3 , 1:6 + 1 drop of gl. HOAc); $^1\text{H NMR}$ ($\text{DMSO}-d_6$): δ 1.85–1.98 (m, 2H, $\text{Glu}\gamma\text{-CH}_2\text{CH}_2$), 2.27–2.32 (m, 2H, $\text{Glu}\gamma\text{-CH}_2\text{CH}_2$), 4.26–4.34 (m, 1H, $\text{Glu}\alpha\text{-CH}$), 5.10–5.14 (d, 2H, Benzylic CH_2), 6.55 (s, H, CH_2NH), 6.55–6.58 (d, 2H, $J=9.0$ Hz, 2 CH), 6.94 (br s, 2H, 2-NH₂ exch), 7.19–7.24 (t, 1H, $J=7.5$ Hz), 7.38–7.40 (d, 1H, $J=7.5$ Hz), 7.56–7.59 (d, 2H, $J=9.0$ Hz), 7.68–7.70 (d, 1H, $J=7.5$ Hz), 7.97–8.00 (d, 1H, $J=6.9$ Hz, NH exch), 11.19 (s, 1H, 3-NH exch), 12.66 (s, 2H, 2COOH exch); HRMS (ESI, pos mode) m/z [$\text{M}+\text{H}^+$] calcd for $\text{C}_{23}\text{H}_{22}\text{N}_5\text{O}_6\text{S}$ 496.1291, found 496.1316.

Table 2
Data collection and refinement statistics for hDHFR-NADPH-6 and 7 ternary complexes

Data collection	hDHFR NADPH-6	hDHFR NADPH-7
PDB accession #	3ntz	3nu0
Space group	H3	H3
Cell dimensions (Å)	84.29 77.79	84.39 78.19
Beamline	SSRL 9-2	SSRL 9-2
Resolution (Å)	1.35	1.35
Wavelength (Å)	0.975	0.975
R _{sym} (%) ^{a,b}	0.061 (0.72)	0.066 (0.45)
R _{merge}	0.053 (0.62)	0.063 (0.39)
Completeness (%) ^a	100.0 (100.0)	100.0 (100.0)
Observed reflections	169,016	569,239
Unique reflections	45,260	45,587
I/σ(I)	15.3 (1.6)	27.0 (8.6)
Multiplicity ^a	3.7 (3.7)	12.5 (12.1)
Refinement and model quality		
Resolution range (Å)	26.6–1.35	33.1–1.35
No. of reflections	45,259	45,587
R-factor ^c	18.6	18.0
R _{free} -factor ^d	20.5	20.9
Total protein atoms	1817	1868
Total water atoms	164	187
Average B-factor (Å ²)	18.9	15.7
Rms deviation from ideal		
Bond lengths (Å)	0.031	0.035
Bond angles (°)	2.84	2.99
Luzzati	0.159	0.145
Ramachandran plot		
Most favored regions (%)	97.8	97.8
Additional allowed regions (%)	2.2	2.2
Generously allowed regions (%)	0.0	0.0
Disallowed regions (%)	0.0	0.0

^a The values in parentheses refer to data in the highest resolution shell.

^b $R_{sym} = \sum_h \sum_i |I_{h,i} - \langle I_h \rangle| / \sum_h \sum_i I_{h,i}$, where $\langle I_h \rangle$ is the mean intensity of a set of equivalent reflections.

^c R-factor = $\sum |F_{obsd} - F_{calcd}| / \sum F_{obsd}$, where F_{obsd} and F_{calcd} are observed and calculated structure factor amplitudes.

^d R_{free}-factor was calculated for R-factor for a random 5% subset of all reflections.

6.14.4. (2S)-2-(5-[(2-Amino-4-oxo-3,4-dihydro[1]benzothieno[2,3-d]pyrimidin-5-yl)methyl]amino)-1-oxo-1,3-dihydro-2H-isoindol-2-yl)pentanedioic acid (7)

Using the general procedure described above with **16** and **22** afforded **7** (40 mg, 32%) as a orange solid; mp >300 °C; R_f 0.27 (MeOH/EtOAc, 1:6); R_f 0.30 (MeOH/CHCl₃, 1:6 + 1 drop of NEt₃); R_f 0.33 (MeOH/CHCl₃, 1:6 + 1 drop of gl. HOAc); ¹H NMR (DMSO-*d*₆): δ 1.97–2.20 (m, 4H, Gluβ-CH₂, Gluγ-CH₂), 4.21–4.25 (m, 2H, isoindoliny CH₂), 4.68–4.71 (m, 1H, Gluα-CH), 5.13, 5.14 (d, 2H, benzylic CH₂), 6.64 (br s, 2H, C₆H₃), 6.74 (s, 1H, NH exch), 6.89 (s, 2H, 2-NH₂ exch), 7.20–7.26 (t, 1H, J = 7.5 Hz, C₆H₃), 7.30–7.33 (d, 1H, J = 8.0 Hz, C₆H₃), 7.39–7.42 (dd, 1H, C₆H₃), 7.69–7.72 (d, 1H, J = 8.0 Hz, C₆H₃), 11.11 (s, 1H, 3-NH exch), 12.78 (s, 2H, 2COOH exch). HRMS (ESI, pos mode) *m/z* [M+H⁺] calcd for C₂₄H₂₁N₅O₆S, 508.1285; found, 508.1321.

6.15. Structure determination and refinement

Expression and purification of hDHFR were carried out as previously described.⁴⁰ Recombinant hDHFR was washed in a Centri-con-10 with 10 mM HEPES buffer, pH 7.4, and concentrated to 11.9–12.1 mg/mL for the two samples. The hDHFR protein was incubated with NADPH and an excess of compounds **6** and **7** for 1 h over ice prior to crystallization using the hanging drop vapor diffusion method. The reservoir solution for inhibitor **6** contained 100 mM KPO₄, pH 6.9, 66% saturated NH₄SO₄, 3% v/v ethanol and 70% saturated NH₄SO₄ for compound **7**. Crystals of hDHFR complex grew over several days at 14 °C and were trigonal, space group H3.

Data were collected to 1.35 Å resolution for both complexes using the remote access robot^{46–48} at liquid N₂ temperatures on beamline 9–2 at the Stanford Synchrotron Research Laboratory (SSRL) imaging plate system. The data were processed using Mosflm.⁴⁹ The diffraction statistics are shown in Table 2 for the two complexes.

The structures were solved by molecular replacement methods using the coordinates for hDHFR (u072) in the program Molref.⁴⁹ Inspection of the resulting difference electron density maps made using the program COOT⁵⁰ running on a MacG5 workstation revealed density for the ternary complex in both crystals. The final cycles of refinement were carried out using the program Refmac5 in the CCP4 suite of programs. The Ramachandran conformational parameters from the last cycle of refinement generated by PROCHECK⁵¹ showed that more than 98% of the residues have the most favored conformation and none are in the disallowed regions. Coordinated for these structures have been deposited with the Protein Data Bank (3ntz, 3nu0).

6.16. Dihydrofolate reductase (DHFR) assay⁵²

All enzymes were assayed spectrophotometrically in a solution containing 50 μM dihydrofolate, 80 μM NADPH, 50 mM Tris-HCl, 0.001 M 2-mercaptoethanol, and 0.001 M EDTA at pH 7.4 at 30 °C. The reaction was initiated with an amount of enzymes yielding a change in optical density at 340 nm of 0.015 units/min.

6.17. Thymidylate synthase (TS) assay

TS was assayed spectrophotometrically at 30 °C and pH 7.4 in a mixture containing 0.1 M 2-mercaptoethanol, 0.0003 M (6*R,S*)-tetrahydrofolate, 0.012 M formaldehyde, 0.02 M MgCl₂, 0.001 M dUMP, 0.04 M Tris-HCl, and 0.00075 M NaEDTA. This was the assay described by Wahba and Friedkin⁵³ except that the dUMP concentration was increased 25-fold according to the method of Davisson et al.⁵⁴ The reaction was initiated by the addition of an amount of enzyme yielding a change in absorbance at 340 nm of 0.016 units/min in the absence of inhibitor.

Acknowledgments

This work is supported by National of Institute of Health, National Institute of Allergy and Infectious Diseases grant A1069966 (A.G.), National Cancer Institute grant CA 125153 (A.G.) and General Medical Institute grant GM051670 (V.C.). The National Science Foundation, CHE0614785, is acknowledged for NMR facilities.

Supplementary data

Supplementary data (Elemental analysis and High-Resolution Mass Spectra (HRMS) (EI)) associated with this article can be found, in the online version, at doi:10.1016/j.bmc.2011.03.067.

References and notes

- Jackson, R. C. *Antifolate Drugs in Cancer Therapy*. Jackman, A. L., Ed.; Humana Press: Totowa, 1999, pp 1–12.
- Gangjee, A.; Elzein, E.; Kothare, M.; Vasudevan *Curr. Pharm. Des.* **1996**, *2*, 263–280.
- DeGraw, J. I.; Colwell, W. T.; Piper, J. R.; Sirotiak, F. M.; Smith, R. L. *Curr. Med. Chem.* **1995**, *2*, 630–653.
- Huenekens, F. M.; Duffy, T. H.; Vitols, K. S. *NCl monogr.* **1987**, *5*, 1–8.
- Berman, E. M.; Werbel, L. M. *J. Med. Chem.* **1991**, *34*, 479–485.
- Chu, E.; Callender, M. A.; Farrell, M. P.; Schmitz, J. C. *Cancer Chemother. Pharmacol.* **2003**, *80*–897.
- Danenber, P. V. *Biochim. Biophys. Acta* **1977**, *47*, 73–92.
- Hitchings, G. H. *Functions of Tetrahydrofolate and the Role of Dihydrofolate Reductase. In Cellular Metabolism in Inhibition of Folate Metabolism in Chemotherapy*; Hitchings, G. H., Ed.; Springer: New York, 1983, pp 11–23.

9. Jackman, A. L.; Taylor, G. A.; Gibson, W.; Kimbell, R.; Brown, M.; Calvert, A. H.; Judson, I. R.; Hughes, L. R. *Cancer Res.* **1991**, *51*, 5579–5586.
10. Taylor, E. C.; Kuhnt, D.; Shih, C.; Rinzal, S. M.; Grindey, G. B.; Barredo, J.; Jannatipour, M.; Moran, R. *J. Med. Chem.* **1992**, *35*, 4450–4454.
11. Bertino, J. R.; Kamen, B.; Romanini, A. Folate Antagonists. In *Cancer Medicine*; Holland, J. F., Frei, E., Bast, R. C., Kufe, D. W., Morton, D. L., Weichselbaum, R. R., Eds.; Williams and Wilkins: Baltimore, MD, 1997; Vol. 1, pp 907–921.
12. Gibson, W.; Bisset, G. M. F.; Marsham, P. R.; Kelland, L. R.; Judson, I. R.; Jackman, A. L. *Biochem. Pharmacol.* **1993**, *45*, 863–869.
13. Sikora, E.; Jackman, A. L.; Newell, D. F.; Calvert, A. H. *Biochem. Pharmacol.* **1988**, *37*, 4047–4054.
14. Jackman, A. L.; Newell, D. R.; Gibson, W.; Jodrell, D. I.; Taylor, G. A.; Bishop, J. A.; Hughes, L. R.; Calvert, A. H. *Biochem. Pharmacol.* **1991**, *42*, 1885–1895.
15. Nair, M. G.; Abraham, A.; McGuire, J. J.; Kisliuk, R. L.; Galivan, J. H.; Ferone, R. *Cell. Pharmacol.* **1994**, *1*, 245–249.
16. Bisset, G. M. F.; Bavetsias, V.; Thornton, T. J.; Pawelczak, K.; Calvert, A. H.; Hughes, L. R.; Jackman, A. L. *J. Med. Chem.* **1994**, *37*, 3294–3302.
17. Barakat, R. R.; Li, W. W.; Lovelace, C.; Bertino, J. R. *Gynecol. Oncol.* **1993**, *51*, 54–60.
18. McCloskey, D. E.; McGuire, J. J.; Russell, C. A.; Rowan, B. G.; Bertino, J. R.; Pizzorno, G.; Mini, E. *J. Biol. Chem.* **1991**, *266*, 6181–6187.
19. Braakhuis, B. J. M.; Jansen, G.; Noordhuis, P.; Kegel, A.; Peters, G. J. *Biochem. Pharmacol.* **1993**, *46*, 2155–2161.
20. Gangjee, A.; Devraj, R.; McGuire, J. J.; Kisliuk, R. L. *J. Med. Chem.* **1995**, *38*, 4495–4502.
21. Marsham, P. R.; Jackman, A. L.; Barker, A. J.; Boyle, F. T.; Pegg, S. J.; Wardleworth, J. M.; Kimbell, R.; O'Connor, B. M.; Calvert, A. H.; Hughes, L. R. *J. Med. Chem.* **1995**, *38*, 994–1004.
22. Tripos Inc., 1699 South Hanley Road, St. Louis, MO 63144.
23. Pendergast, W.; Dickerson, S. H.; Dev, I. K.; Ferone, R.; Duch, D. S.; Smith, G. K. *J. Med. Chem.* **1994**, *37*, 838–844.
24. Beutel, G.; Glen, H.; Schoffski, P.; Chick, J.; Gill, S.; Cassidy, J.; Twelves, C. *Clin Cancer Res.* **2005**, *11*, 5487–5495.
25. Dev, I. K.; Dallas, W. S.; Ferone, R.; Hanlon, M.; McKee, D. D.; Yates, B. B. *J. Biol. Chem.* **1994**, *269*, 1873–1882.
26. Hooijberg, J. H.; Broxterman, H. J.; Kool, M.; Assaraf, Y. G.; Peters, G. J.; Noordhuis, P.; Scheper, R. J.; Borst, P.; Pinedo, H. M.; Jansen, G. *Cancer Res.* **1999**, *59*, 2532–2535.
27. Montfort, W. R.; Weichsel, A. *Pharmacol. Ther.* **1997**, *76*, 29–43.
28. Stout, T. J.; Stroud, R. M. *Structure* **1996**, *4*, 67–77.
29. Weichsel, A.; Montfort, W. R. *Nat. Struct. Biol.* **1995**, *2*, 1095–1101.
30. Weichsel, A.; Montfort, W. R.; Ciesla, J.; Maley, F. *Proc. Natl. Acad. Sci.* **1995**, *92*, 3493–3497.
31. Vainio, M. J.; Johnson, M. S. *J. Chem. Inf. Model.* **2007**, *47*, 2462–2474.
32. Gewalt, K.; Schinke, E.; Böttcher, H. *Chem. Ber.* **1966**, *99*, 94–100.
33. Zhang, M.; Harper, R. W. *Bioorg. Med. Chem. Lett.* **1997**, *7*, 1629–1634.
34. Rosowsky, A.; Chen, K. K.; Lin, M. *J. Med. Chem.* **1973**, *16*, 191–194.
35. Gangjee, A.; Yu, J. M.; Copper, J. E.; Smith, C. D. *J. Med. Chem.* **2007**, *50*, 3290–3301.
36. Yadav, P. P.; Gupta, P.; Chaturvedi, A. K.; Shukla, P. K.; Maurya, R. *Bioorg. Med. Chem.* **2005**, *13*, 1497–1505.
37. Sengupta, S. K.; Chatterjee, S.; Protopapa, H. K.; Modeat, E. J. *J. Org. Chem.* **1972**, *37*, 1323–1328.
38. Wartenberg, F. H.; Koppe, T.; Wetzel, W.; Wydra, M.; Benz, A., PCT Int. Appl.(2001), CODEN: PIXXD2 WO 01/77099 A1 19980305.
39. Rosowsky, A.; Forsch, R. A.; Null, A.; Moran, R. G. *J. Med. Chem.* **1999**, *42*, 3510–3519.
40. Patil, S. D.; Jones, C.; Nair, M. G.; Galivan, J.; Maley, F.; Kisliuk, R. L.; Gaumont, Y.; Duch, D.; Ferone, R. *J. Med. Chem.* **1989**, *32*, 1284–1289.
41. Hughes, L. R.; Jackman, A. L.; Oldfield, J.; Smith, R. C.; Burrows, K. D.; Marsham, P. R.; Bishop, J. A. M.; Jones, T. R.; O'Connor, B. M.; Calvert, A. H. *J. Med. Chem.* **1990**, *33*, 3060–3067.
42. Marsham, P. R.; Jackman, A. L.; Hayter, A. J.; Daw, M. R.; Snowden, J. L.; O'Connor, B. M.; Bishop, J. A.; Calvert, A. H.; Hughes, L. R. *J. Med. Chem.* **1991**, *34*, 2209–2218.
43. Gangjee, A.; Li, W.; Kisliuk, R. L.; Cody, V.; Pace, J.; Piraino, J.; Makin, J. *J. Med. Chem.* **2009**, *52*, 4892–4902.
44. Cody, V.; Luft, J. R.; Pangborn, W. *Acta Crystallogr., Sect. D: Biol. Crystallogr.* **2005**, *61*, 147–155.
45. DELano Scientific LLC, PyMol.
46. McPhillips, T. M.; McPhillips, S. E.; Chiu, H. J.; Cohen, A. E.; Deacon, A. M.; Ellis, P. J.; Garman, E.; Gonzalez, A.; Sauter, N. K.; Phizackerley, R. P.; Soltis, S. M.; Kuhn, P. *J. Synchrotron Radiat.* **2002**, *9*, 401–406.
47. Cohen, A. E.; Ellis, P. J.; Miller, M. D.; Deacon, A. M.; Phizackerley, R. P. *J. Appl. Crystallogr.* **2002**, *35*, 720–726.
48. Gonzalez, A.; Moorhead, P.; McPhillips, S. E.; Song, J.; Sharp, K.; Taylor, J. R.; Adams, P. D.; Sauter, N. K.; Soltis, S. M. *J. Appl. Crystallogr.* **2008**, *41*, 176–184.
49. Collaborative Computational Project, Number 4. The CCP4 suite: programs for protein crystallography. *Acta Crystallogr., Sect D* **1994**, *50*, 760–763.
50. Emsley, P.; Cowtan, K. *Acta Crystallogr., Sect D* **2004**, *60*, 2126–2132.
51. Laskowski, R. A.; MacArthur, M. W.; Moss, D. S.; Thornton, J. M. *J. Appl. Crystallogr.* **1993**, *26*, 283–291.
52. Kisliuk, R. L.; Strumpf, D.; Gaumont, Y.; Leary, R. P.; Plante, L. *J. Med. Chem.* **1977**, *20*, 1531–1533.
53. Wahba, A. J.; Friedkin, M. *J. Biol. Chem.* **1962**, *237*, 3794–3801.
54. Davisson, V. J.; Sirawaraporn, W.; Santi, D. V. *J. Biol. Chem.* **1989**, *264*, 9145–9148.